

Influence of Toroidicity on Reversed Field Pinch Dynamics

W.J.T. Bos¹, J.A. Morales², K. Schneider³ and D.C. Montgomery⁴

¹ *LMFA, CNRS, École Centrale de Lyon, France*

² *CEA / IRFM, Cadarache, Saint-Paul-Lez-Durance, France*

³ *M2P2, CMI, CNRS, Aix-Marseille Université, France*

⁴ *Department of Physics and Astronomy, Dartmouth College, NH, USA*

The Reversed Field Pinch (RFP) possesses the technical advantage that the imposed toroidal magnetic field needs not to be as large as for a tokamak. However, it was shown that RFP devices are plagued by magnetohydrodynamic (MHD) instabilities, leading to a turbulent state which degrades the confinement quality. However, in the last two decades quasi-single helicity (QSH) states were observed in RFP experiments, where the full turbulent regime is avoided and one helical mode predominates [1, 2, 3, 4]. In the QSH state there is a decrease of magnetic chaos and the formation of a coherent helical structure within the plasma.

In this study we investigate the influence of the curvature of the magnetic field on the RFP dynamics by comparing two distinct geometries: a torus with a periodic cylinder. It is found that an axisymmetric toroidal mode is always present in the toroidal, but absent in the cylindrical configuration. In particular, in contrast to the cylinder, the toroidal case presents a double poloidal recirculation cell with a shear localized at the plasma edge. Quasi-single-helicity states are found to be more persistent in toroidal geometry than in periodic cylinder. Also quantitatively, better agreement in the decrease of the magnetic toroidal field at the edge, as a function of the pinch parameter is observed for the toroidal geometry simulations rather than for the straight cylinder case.

We consider non-ideal MHD in which both viscous and resistive effects are taken into account. Indeed, if we drop the resistive term and consider ideal MHD, the imposed toroidal electric field will become independent from the toroidal plasma current, an assumption which can dramatically change the plasma dynamics [5]. The Alfvén-normalized MHD equations are,

$$\partial_t \mathbf{u} - M^{-1} \nabla^2 \mathbf{u} = -\nabla p^* + \mathbf{u} \times \boldsymbol{\omega} + \mathbf{j} \times \mathbf{B}, \quad (1)$$

$$\partial_t \mathbf{B} - S^{-1} \nabla^2 \mathbf{B} = \nabla \times (\mathbf{u} \times \mathbf{B}), \quad (2)$$

with $\nabla \cdot \mathbf{u} = 0$ and $\nabla \cdot \mathbf{B} = 0$, the current density $\mathbf{j} = \nabla \times \mathbf{B}$, the vorticity $\boldsymbol{\omega} = \nabla \times \mathbf{u}$, the total pressure $p^* = p + u^2/2$. Two distinct geometries are considered: a torus and a periodic cylinder, both with circular cross-section. The reference length L is the diameter of these cross sections. The normalization introduces two dimensionless quantities, $S = C_A L / \lambda$ and $M = C_A L / \nu$ the

Lundquist and Montgomery number, respectively, with λ the magnetic diffusivity and ν the kinematic viscosity. The ratio of these two quantities is the magnetic Prandtl number $Pr = \nu/\lambda$.

For a given geometry, the helical curvature of the magnetic field is in our system determined by the pinch ratio Θ . For the toroidal geometry the Θ parameter is defined as the wall averaged poloidal magnetic field over the volume averaged toroidal magnetic field, $\Theta = \overline{B_P}/\langle B_T \rangle$. For the periodic cylinder B_T needs to be replaced by B_Z in this definition.

Toroidal and cylindrical helical states

For the considered geometry, under our assumptions, the dynamics are entirely determined by the parameters M , Pr and Θ . In the present investigation we keep the magnetic Prandtl number fixed at $Pr = 3$ and we consider two different Montgomery numbers $M = 444$ and $M = 888$. Here we shall focus in particular on the influence of the pinch ratio on the dynamics. All results are evaluated once the system has obtained a statistically steady state.

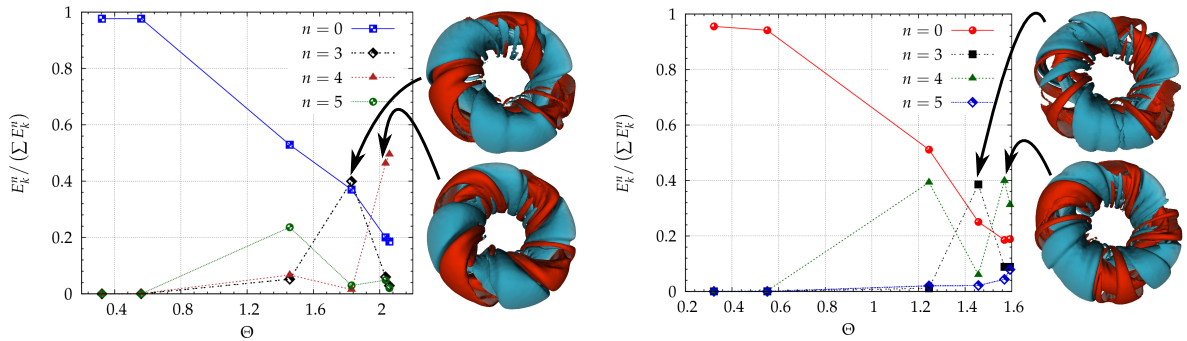


Figure 1: Ratio of the kinetic energy of the dominant toroidal modes over the total kinetic energy for the torus geometry, $M = 444$ (left) and $M = 888$ (right) as a function of Θ . Visualization of the modes: toroidal velocity isocontours $+0.007$ (blue) and -0.007 (orange).

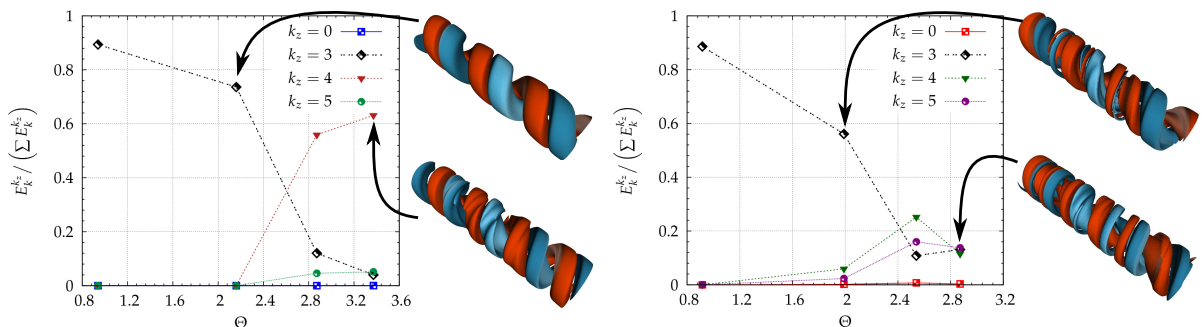


Figure 2: Ratio of the kinetic energy of the dominant axial modes over the total kinetic energy for the cylindrical geometry, $M = 444$ (left) and $M = 888$ (right) as a function of Θ . Visualization of the modes: axial velocity isocontours $+0.008$ (blue) and -0.008 (orange).

In Fig. 1 it is shown that for a value of $\Theta < 1$ the kinetic energy is mostly contained in the zero toroidal mode. This means that the velocity field for these parameters is axi-symmetric around the major axis of the torus. At higher values of Θ , roughly around $\Theta = 1$, the helical modes with $n \neq 0$ become important. But even at the highest values of Θ reported in the present

investigation, the toroidal zero mode represents around 20% of the total kinetic energy and thus importantly affects the dynamics for all cases considered here. In contrast, in the cylindrical geometry the relative influence of the axial-invariant mode is negligible for all values of M and Θ . This marks an important difference: due to the curvature of the magnetic field, RFP dynamics will always be governed by a mix of helical modes, and toroidally invariant modes. These latter are absent in cylindrical geometry.

The dominant helical modes at the higher pinch ratios are n or $k_z = 3, 4$ for the toroidal and cylindrical geometry (see Figs. 1 and 2). This result is in good agreement with experimental data from the RFP RELAX, which possesses an aspect ratio ~ 2 close to one in the present simulations. The dominant modes measured in this device are $n = 4$ and $n = 5$ [7]. For the simulations performed with $M = 888$ there is an equipartition of the kinetic energy between more modes in the cylindrical geometry and the state is in a multiple-helicity state [1]. The toroidal simulations have a mode $n = 4$ which continues to be significantly more energetic than the others. The toroidal geometry displays thus a state closer to a single-helicity state than the cylinder.

In Fig. 3 (a), an instantaneous plot of the velocity field in a poloidal cross section is presented for the simulation with $M = 444$ and $\Theta = 1.83$. Fig. 3 (b) shows the toroidally averaged poloidal flow, corresponding to the $n = 0$ mode. This field is composed of two counter-rotating vortices, and is characterized by peaked poloidal velocities located in the external region where a shear zone exists. The kinetic energy of the zero mode is mainly localized at the plasma edge. This flow-field was obtained analytically for large transport coefficients in [8] and numerically for relatively high Lundquist numbers in [9]. In Fig. 3 (c) we show the flow corresponding to the helical modes modes $n \neq 0$, the dominant mode is $n = 3$. If the total poloidal flow is compared to the poloidal flow in the cylindrical geometry Fig. 3 (d), an important difference is observed. The double vortex flow pattern appearing in the torus is completely absent in the cylindrical geometry. This poloidal flow pattern is relevant because the flow is composed of two counter-rotating vortices with the shear at the plasma edge. This steep gradient zone could be related to transport barriers that are observed experimentally [10]. It seems from the present results that this flow pattern might be related to MHD self-organization, but only in the presence of a toroidally curved magnetic field.

Quantitatively the numerical results are compared to experimental data of three different RFP devices. The first set of experimental data comes from the REPUTE experiment, that is described in [11], the second set of data is the RFP ZT-40M [11] and the third is from the device RELAX [7]. We recall that this last experiment has a low aspect ratio ~ 2 , close to the aspect

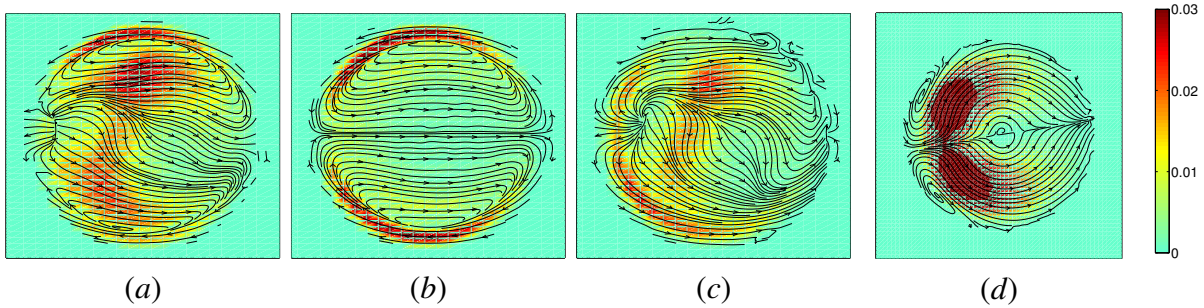


Figure 3: Poloidal velocity vector norm (color) and poloidal streamlines in the toroidal geometry (a-c) and cylinder (d). (a) – Total poloidal velocity field in a poloidal cut. (b) – The azimuthally averaged poloidal field (mode $n = 0$). (c) – The total field (a) minus the azimuthally averaged field (b). For $M = 444$ and $\Theta = 1.83$. (d) – Total poloidal velocity field in a poloidal cut in the cylinder for $M = 444$ and $\Theta = 2.16$.

ratio used in the present simulations. In Fig. 4 our numerical and the experimental results are presented in the $\Theta - F$ plane. F is the reversal parameter defined as the wall averaged toroidal magnetic field over the volume averaged toroidal magnetic field, $F = \overline{B_T}/\langle B_T \rangle$.

From Fig. 4 we can see that the simulations give results in the $\Theta - F$ plane comparable to those obtained in the RFP experiments: The reversal of the toroidal magnetic field B_T for the considered experiments occurs around the same value, for $\Theta \approx 1.5$. The set of simulations that fits best the experiments is the one performed for a toroidal geometry with viscous Lundquist number $M = 888$. In this figure we note that both the geometry and the Lundquist number play an important role in the evolution of the reversal parameter F with Θ . Using the toroidal geometry and increasing sufficiently the viscous Lundquist number, we fit better the experimental data.

References

- [1] D. Escande *et al.*, Phys. Rev. Lett. **85**, 8 (2000)
- [2] P. Brunsell *et al.*, Phys. Fluids B **5**, 885 (1993)
- [3] P. Martin *et al.*, Phys. Plasmas **7**, 5 (2000)
- [4] R. Lorenzini *et al.*, Nature Physics **5**, 8 (2009)
- [5] D.C. Montgomery and X. Shan, Comments Plasma Phys. Control. Fusion **15**, 315 (1994)
- [6] D.C. Montgomery *et al.*, Phys. of Plasmas **4**, 4 (1997)
- [7] R. Ikezoe *et al.*, Plasma Phys. Control. Fusion **53**, 2 (2011)
- [8] J.W. Bates and D.C. Montgomery , Phys. of Plasmas **5**, 2649 (1998)
- [9] J.A. Morales *et al.*, Phys. Rev. Lett. **109**, 17 (2012)
- [10] M.E. Puiatti *et al.*, Nucl. Fusion **51**, 7 (2011)
- [11] J.B. Taylor, Reviews of Modern Phys. **58**, 3 (1986)

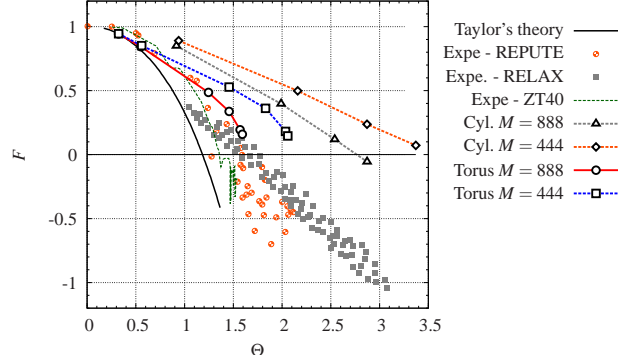


Figure 4: Field reversal parameter F as a function of the pinch parameter Θ for the toroidal and cylindrical simulations and experimental data of three RFP devices.